Microstructural Development in an Ammonium-based Partial Melt System

Youngdo Park

Department of Earth and Environmental Sciences

Korea University, Anam-dong, Sungbuk-ku, Seoul 136-701, Korea

email: ydpark@kuccnx.korea.ac.kr,

fax: +82 2 927 6180

Table of contents

Previous Section Home Next Section

Park, Y. 2000. Microstructural Development in an Ammonium-based Partial Melt System. In: Stress, Strain and Structure, A volume in honour of W. D. Means. Eds: M.W. Jessell and J.L.Urai. Volume 2, Journal of the Virtual Explorer. ISSN 1441-8126 (Print). ISSN 1441-8134 (CD-ROM). ISSN 1441-8126 (On-line at www.virtualexplorer.com.au/VEjournal/Volume2).

Abstract

Microstructural development in a rock analog partial melt system is experimentally studied with the technique of synkinematic microscopy in which crystal-scale processes can be inferred after direct observation of microstructural changes. The aim of this work is to establish the link between microstructural changes and processes. Textural metamorphism such as dendrite segmentation, coarsening, and grain- or phase-boundary migration, is observed in the analog system even at supersolidus conditions. These processes may introduce complications when attempting to interpret the igneous textures since a great portion of textures in igneous rocks can be modified by textural metamorphism. During deformation experiments of the partial melt systems, microstructures indicating crystal plasticity and dynamic recrystallization are observed at faster strain rates (~10% per hour) and the resulting microstructures are similar to those formed at solid-state conditions. At slow strain rates (~1% per hour), a pressure solution-like process, contact melting, is active, resulting in optically strain-free crystals. Sliding along crystal boundaries is active in both regimes of strain rates. The observed microstructural development also introduces difficulties when interpreting deformation in igneous rocks; deformation microstructures indicating crystal plasticity can be formed at supersolidus and subsolidus conditions, and igneous rocks with optically strain-free crystals may have undergone large deformation by contact melting and sliding.

Previous Section Home Next Section

Introduction

Textures in igneous rocks may record process histories during evolution of igneous rocks. For example, deformation processes and the types of deformation in magma chambers can be interpreted by studying igneous fabrics (e.g. Paterson et al, 1991), and the relative rates of nucleation and crystal growth can be inferred by observing crystal size distributions (CSDs) of igneous rocks (e.g. Cashman and Marsh, 1988). In spite of these benefits from textural studies in igneous rocks, texture-based interpretations on processes and conditions have been unreliable or difficult due to a lack of thorough knowledge of the links between processes and textures. This is partly because of the slow kinetics of processes in silicate melts, which makes it difficult or impossible to simulate natural processes in experiments as discussed by McBirney (1993).

Experiments using an artificial magmatic system were carried out in this study with the purpose of strengthening the links between processes and textures. The experimental technique of synkinematic microscopy was employed, since textural development at any instant can be observed and recorded so that textural development and related processes can be incorporated into the interpretation of final textures instead of the textural development being guessed.

Fourteen time-lapse movies obtained from the experiments on the artificial magmatic system will be discussed. The movies consist of two groups. The first group of the movies is about textural development at zero strain rate, and the second group is about the textural development during deformation. Much of the description of the movies discussed in this paper is given by Means and Park (1994), Park (1994), Park & Means (1996), and Park & Means (1997).

Experiments

Sample Material

The experimental magmatic system consists of three crystalline phases and melt (Figure 1a). The crystalline phases are ammonium thiocyanate - NH_4SCN (W in Figure 1a, white phase hereafter), ammonium chloride - NH_4Cl (C in Figure 1a, cube phase hereafter), and diammonia tetrathiocyanato cobaltate - $(NH_4)_2[Co(SCN)_4]nH_2O$ (B in Figure 1a, blue phase hereafter). The liquid phase (M in Figure 1a) is a hydrous solution with dissolved ions of NH_4^+, Cl^-, SCN^- and $[Co(SCN)_4]^{2-}$. The physical, optical and petrographic properties are given in Figure 1b and details about the procedures of sample preparation are described in Means and Park (1994).

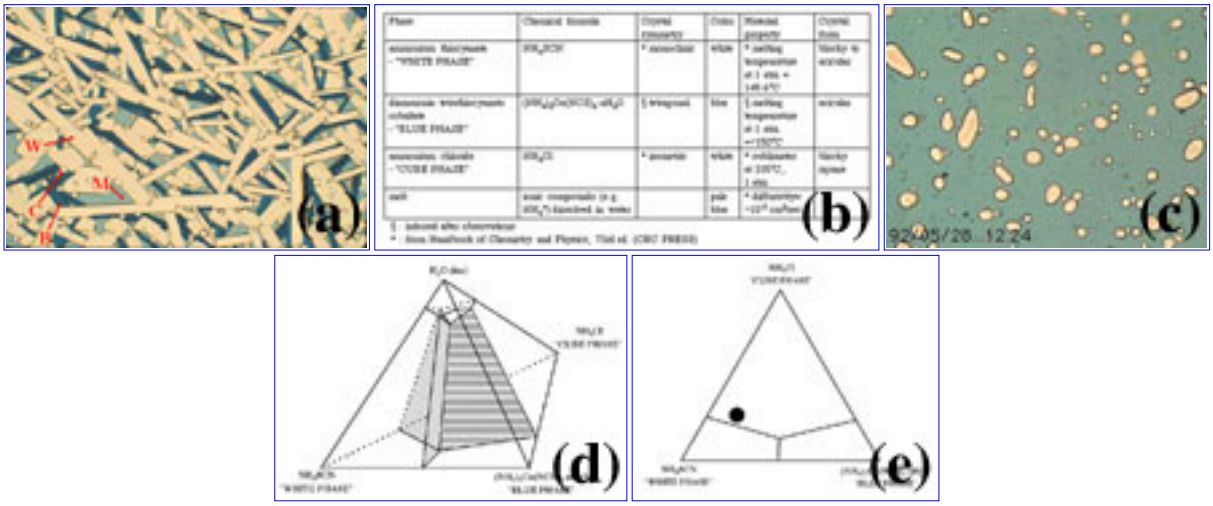

Figure 1. Phase relations of the experimental magmatic melt system. (a) photomicrograph of the sample material (W: white phase, C: cube phase, B: blue phase, M: melt). Plane-polarized light. Field width: 1.5mm. (b) properties of the phases. (c) crystallization sequence of the experimental material from 60ºC to 31ºC at a cooling rate of 5ºC per hour. Plane-polarized light. Field width: 0.6mm. (d) a quaternary eutectic phase diagram for the experimental magmatic system. (e) bulk composition (closed circle) of the experimental system on a white-cube-blue phase section of the quaternary eutectic diagram.

Figure 1c shows the crystallization sequence of the bulk composition used in this study. The first-crystallizing phase (thus liquidus phase) is the cube phase, although initial crystallization from the crystal-free melt is not shown. Then, white phase crystals nucleate and grow, and finally blue phase crystals appear. The color of melt becomes pale as blue crystals appear at the end of Figure 1c, suggesting the incorporation of the blue $[Co(SCN)_4]^{2-}$ ions of the melt into blue phase crystals. Based on the observation of the appearance and disappearance of the crystals during cooling and melting experiments, and the observation that the crystalline phases do not react with melt and produce a new crystalline phase, a quaternary eutectic phase diagram (Figure 1d) is constructed for the experimental system. The bulk composition of the experimental system is shown on the section parallel to the plane of the cube-white-blue phase (Figure 1e).

Experimental Apparatus

The experimental apparatus used in this study is shown in Figure 2a. A mini-press designed

by Janos Urai is attached on the stage of a petrographic microscope (Figure 2b and c) and a 35mm camera and a video camera attached to a Macintosh through a frame grabber are mounted on a microscope for recording the experimental images. Temperature conditions during experiments were set up by a programmable temperature controller (Eurothem model 808) for different types of the thermal histories (e.g. constant temperature, cooling and cycling). A Macintosh utility, QuicKeys, was used when recording the zero strain-rate experiments while unattended.

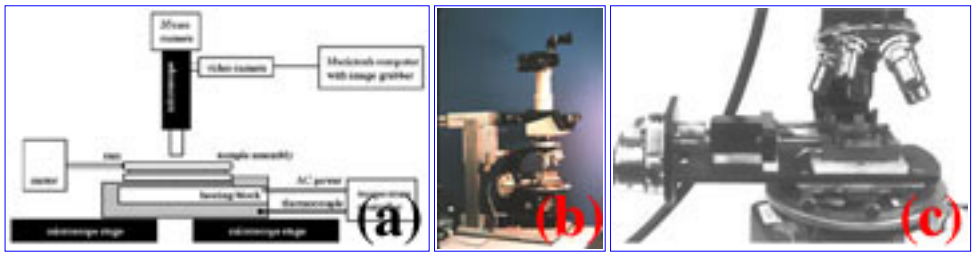

Figure 2. Experimental apparatus used in this study. (a) schematic diagram illustrating the overall experimental apparatus. (b) Urai-press mounted petrographic microscope. (c) Close-up photograph of the Urai press (from Ree, 1991)

The experimental samples were prepared using a sets of glass slides on which scratches were made using a glass-cutting pen. Thicker crystals grow from the melt into the scratched area of the glass slides and they serve as grips to cause deformation in the area between scratches (Figure 3a). The scratch geometries used for deformation experiments are pure shearing (Figure 3b), simple shearing (Figure 3c) and general (or mixed) shearing.

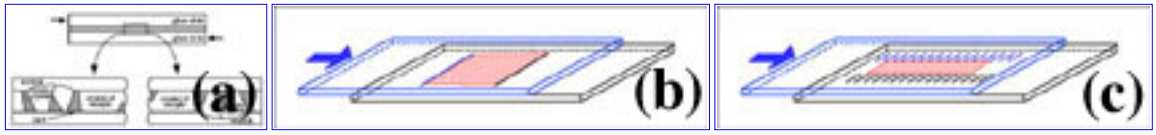

Figure 3. Sample assembly for deformation experiment. (a) Sectional view of the sample and grips where thicker crystals grow. (b) Grip geometry for pure shear deformation. (c) Grip geometry for simple shear deformation.

Previous Section Home Next Section

Microstructural Development at Zero Strain Rate

Segmentation and Coarsening of Dendritic Crystals

Dendrite segmentation is a process by which primary crystals of dendritic form in melt become subdivided into pieces surrounded by melt (Kattamis et al, 1967; Kahlweit, 1968). Dendrite segmentation can therefore be a type of 'nucleation' process. An example is shown in Figure 4a. Conventional interpretation of the last frame in the time-lapse movie of Figure 4a would be that each crystal in the last frame represents one nucleus and larger crystals had a longer growth time or a faster growth rate. However, as shown in the sequence of the time-lapse movie, crystals in the last frame of Figure 4a are not crystals formed by accretion around individual nuclei, but crystals which survived during segmentation of a dendritic crystal and coarsening. The first frame in Figure 4a was taken moments after crystallization of a white phase dendritic crystal. Since a dendritic crystal has a large surface area to volume ratio, it is not stable due to the excessive surface energy and spontaneously breaks down by segmentation. Segmentation of a dendrite, indicated by separated pieces of arms, has already begun at the stage of the first frame. After segmentation, coarsening (or dissolution of smaller crystals and growth of larger crystals) occurs and results in very different texture at the end. Measurements of the interfacial surface over time are shown in Figure 4b. A remarkable decrease in the surface area (in fact, perimeter of crystals) during the first 30 minutes can be seen. The rate of decrease in surface area becomes slower over time, since the driving force, the interfacial surface energy, decreases over time. There is also an apparent volume decrease of crystalline phases during segmentation and coarsening. This is because the initial dendritic crystals do not fully occupy the space between two glass slides while the crystals fully occupy the space after segmentation and coarsening.

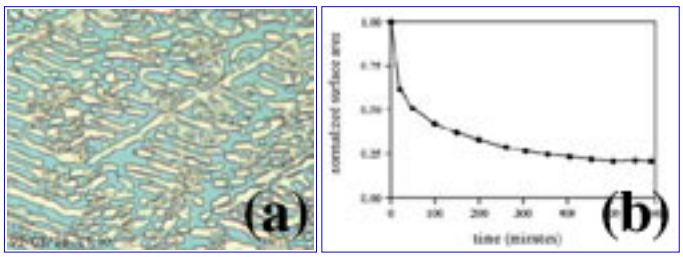

Figure 4. (a) isothermal coarsening of white phase dendritic crystals at 50°C. Plane-polarized light. Field width: 0.4mm. (b) plots of time vs. normalized crystal-melt interfacial area.

Dendritic crystallization is common in cast metals (Rostoker & Dvorak, 1977) and has been found in rapidly cooled experimental silicate systems (Lofgren, 1980). Dendritic crystals also occur in chilled margins of plutons (Shannon et al, 1982; Tegner et al, 1993). Segmentation of dendrites and subsequent coarsening has been known in metallurgy (Kattamis et al, 1967). If segmentation and coarsening of dendrite is possible in silicate systems, this mechanism provides an additional nucleation mechanism, augmenting the conventional nucleation mechanism in which the nucleation rate is the number of nuclei *forming from melt* per volume per time. If segmentation and coarsening lead to formation of 'nuclei' or growth centers around which crystals will grow, the 'nucleation rate' will be, in fact, the sum of a conventional nucleation rate and the rate of growth center formation by dendrite segmentation. This may introduce complications when inferring nucleation rate and growth rate using crystal size distribution (e.g. Cashman & Marsh, 1988).

Grain- and Phase-Boundary Migration

Grain-boundary migration is a process by which a grain boundary between two grains of the same phase migrates to lower the surface free energy or strain energy. Grain-boundary migration is commonly observed in our samples. Figure 5a shows an example of grain-boundary migration between two growing white phase crystals during cooling, resulting in an unexpected change of grain-boundary geometry. The growth-impingement grain boundary (indicated with an arrow) formed between the two white phase crystals in the first frame of Figure 5a starts to migrate and the migrated grain boundary becomes rational with respect to the left white phase crystal in the frames near the end of the time-lapse movie. The order of crystallization, judged from the last frame of Figure 5a, would be such that the left white phase crystal occupied the growth space first, stopped growth and the right white phase crystal formed a growth-impingement boundary. However, the recorded sequence clearly shows the boundary is not a simple impingement boundary but a migrated boundary which has changed its orientation and position. Grain-boundary migration in this example is likely to be driven by surface energy (grain-boundary energy), since strain energy in the lattice is negligibly small because of no concurrent deformation.

Figure 5. Supersolidus grain-boundary migration and phase-boundary migration. (a) grain-boundary migration during cooling (70ºC to 30ºC at a cooling rate of 5ºC per hour). Elapsed time between the first and last frame= 6 hours 20 minutes. Plane-polarized light. Field width: 0.4mm. (b) isothermal phase-boundary migration (50ºC). Elapsed time between the first and last frame= 6 days. Plane-polarized light. Field width: 0.18mm. (c) Possible zonation patterns in crystals after phase-boundary migration. After the formation of normal growth-impingement boundaries between three crystals, the triple junction migrates to the right in order to achieve textural equilibrium. Different types of zonation patterns develop after phase-boundary migration, depending on the range of diffusion.

Phase-boundary migration is a process by which a phase boundary between two phases migrates by chemical reaction or structural transformation. Phase-boundary migration also occurs in this system although the rate is much slower than grain-boundary migration. Figure 5b shows migration of the phase boundary between a blue phase crystal and a white phase crystal, with abundant melt nearby. The blue phase crystal has a square form because its tetragonal c-axis is perpendicular to the plane of the photomicrograph.

During phase-boundary migration between two chemically different phases, transfer of atoms which are involved during chemical reaction is always necessary, unlike grain-boundary migration in which simple detachment and attachment of atoms from one grain to another is necessary. If diffusion along the boundary region is faster than diffusion through the crystals, the boundary region can be viewed as the channel that is connected to a main reservoir of melt during melt-present phase-boundary migration. If diffusion along the boundary is fast or long-range diffusion occurs, the part of a crystal which grows by phase-boundary migration will have a composition in equilibrium with the main melt. However, when only short-range diffusion occurs, the ‘melt’ phase in the boundary region can have a chemistry slightly

different from that of the main melt, and the part of a crystal growing by phase-boundary migration will have an equilibrium composition with the local boundary region ‘melt’. Different mineral zonation patterns will develop depending on the range of diffusion (Figure 5c). Such zonation patterns may be useful when identifying the phase-boundary migration from igneous rocks.

During grain-boundary migration, although melt-connectivity is not required, the grain-boundary region can be also filled with the ‘melt’ of bulk melt composition or local melt composition, depending on the range of diffusion. Similar mineral zonation patterns as in Figure 5c are expected after grain-boundary migration.

Grain Migration through Melt

Grain migration, in polycrystalline aggregates, is accompanied by grain-boundary migration in one direction at the opposite sides of a grain (Fig. 4, Urai et al, 1986). The atoms or material points in a grain where grain migration occurs, however, are fixed in position with respect to the material points outside the grain. Thus, the process of grain migration is markedly different from grain-boundary sliding which requires movement of material points within a grain. A similar process is observed in the experimental magmatic system. The white phase crystals indicated with arrows in Figure 6 migrate by growth at one end and simultaneous dissolution at the other end of the same grain. Dissolution and growth of the white phase crystals can be explained by the local concentration gradient existing between the crystals (migrating and neighboring crystals). The concentration gradient between the crystals is established since the solubility of the crystals (or the equilibrium concentration of the crystals) is dependent on the size of crystals (Gibbs-Thomson equation, Shewmon, 1965).

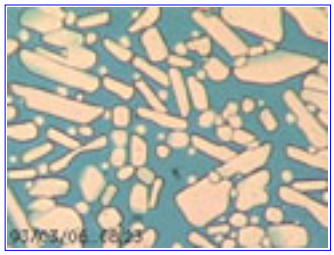

Figure 6. Isothermal grain migration through melt (80ºC). Elapsed time between the first and last frame= 1.5 day. Plane-polarized light. Field width: 0.4mm.

Migration of crystals by grain migration in melt is completely different from the well-known mechanisms such as convection (material transport with medium). The material in crystals that changed their position by grain migration can be much younger than their original nuclei. Zonation patterns in crystals may record grain migration.

Previous Section Home Next Section

Home

Microstructural Development During Deformation

Crystal Plasticity during Fast Strain-Rate Deformation

Crystal plastic deformation by slip inside crystals and dynamic recrystallization is observed during faster strain-rate (~10% per hour) experiments. Sequences of photomicrographs in Figure 7 were taken during a deformation experiment at constant temperature (30^{o}C) and strain rate ~$10^{-4.5}$ shortening per second. The grip geometry used in this experiment was pure shearing with the shortening direction parallel to the horizontal edges of the photomicrographs, although simple shearing between the white phase crystals W1 & W2 is noticeable in the field of view. The white phase crystal W2 (Figure 7) was initially oriented subparallel to the shortening direction. Microstructures developed during crystal plastic deformation of this crystal include progressive bending, as in flexural slip folding, undulose extinction, slip traces in the crystal parallel to the outer rational crystal-melt interface, and possibly cuspy crystal-melt interfaces (indicated by arrows in the last frame of Figure 7). Features similar to the cuspy crystal-melt interface in Figure 7 have been repeatedly observed in other high strain-rate experiments, and sometimes it has been observed that the cuspy interface leads to segmentation of a crystal by tip propagation. The origin of the cuspy crystal-melt interfaces is not clear. One possibility for the development of such structure is that there may be existence of substructures at the cuspy interface. For example, if a subgrain boundary exists, it may lead to development of a cuspy interface, since high defect density near the subgrain boundary can cause increase in solubility. Segmented pieces of crystals (W3 and W4 in Figure 7) which were originally a part of the white phase crystal W2, underwent extensive dynamic recrystallization while interstitial melt was removed by filter pressing. These microstructures formed by dynamic recrystallization are similar to those formed in the solid state, and usually thought of as the result of solid-state deformation (e.g. Paterson et al, 1989).

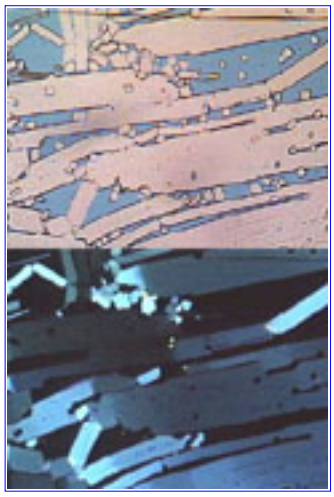

Figure 7. Dynamic recrystallization during melt-present deformation. W1,W2,W3,W4: white phase crystals. Elapsed time between the first and last frame= 14 minutes. Plane- and crossed-polarized light. Field width: 0.47 mm.

Contact Melting during Slow Strain-Rate Deformation

The deformation process of contact melting/redeposition has been observed during slow strain-rate experiments (~$10^{-5.5}$ per second or about an order of magnitude slower than the strain rate at which crystal plasticity is observed). The descriptive term contact

melting/redeposition is used instead of the well established term - pressure solution, since the precise mechanism of dissolution is not known here. Possible causes for dissolution are solubility increase or chemical potential increase due to higher normal stress (Robin, 1978), solubility increase due to stored elastic strain energy in a crystal (Sprunt & Nur, 1977), and solubility increase due to high defect density (Bosworth, 1981; Lasaga, 1981).

Contrary to strain accommodation by bending of a crystal whose long dimension was subparallel to the shortening direction during faster strain-rate experiments (Figure 7), strain accommodation by contact melting occurs, when strain rate is slow enough, by shortening of a crystal by melting at its end(s) or boundaries facing the shortening direction. This is observed in crystal W1 in Figure 8 oriented similarly to the crystal in Figure 7. This crystal shows length decrease by contact melting at its contacts with crystals, W2 and/or W3. Since there is not sufficient bending or bulging to account for the shortening in the white phase crystal W1, the interpretation of crystal length decrease without crystal plastic deformation seems reasonable. The local strain accommodated by contact melting of the white phase crystal W1 is approximately 30% shortening (Figure 8). Slight bending of the white phase crystal W1 (near the last frame of Figure 8) may have driven the grain-boundary migration which led to dissection of the white phase crystal W1 by W4.

Figure 8. Contact melting/redeposition during slow strain-rate experiment. W1,W2,W3,W4,W5,W6,W7: white phase crystals. Elapsed time between the first and last frame= 180 minutes. Plane- and crossed-polarized light. Field width: 0.48 mm.

Contact melting at phase boundaries (boundaries between two different phases) is also observed in Figure 8. The white phase crystal W5 in Figure 8 is forming phase boundaries (in the second frame of Figure 8) with two cube phase crystals (indicated with arrows) by displacement of the cube phase crystals relative to the white phase crystal W5. After further shortening, the two cube crystals initially separated by the white phase crystal W5, are touching each other and forming a displacement-impingement boundary. This seems to be the result of melting of the white phase crystal W5 at the phase boundaries instead of crystal plastic deformation, since no length increase in W5 is observed. Different ability for contact melting for different solid phases can be inferred since the cube phase crystals do not change their crystal shape during contact melting of the white phase crystal W5. Such preferential dissolution by contact melting on one side of a boundary also occurs at grain boundaries. An example of an indented grain boundary produced by preferential contact melting is shown by the white phase crystal W6 in the last frame of Figure 8. This type of microstructure may be useful to identify the process of contact melting/redeposition.

Another example of contact melting/redeposition is shown in Figure 9a. Contact between the blue phase crystal B1 and the white phase crystal W1 was initially a point contact formed by growth of the two crystals. The point contact becomes wider as deformation progresses and this is the result of dissolution of the white phase crystal W1 at the contact. The dissolved constituents from the crystals will result in local increase in the concentration of the constituents, and this will lead to crystallization or redeposition somewhere else in order to maintain chemical equilibrium. Such a process can be observed in the white phase crystals bordering local melt pockets (e.g. white phase crystal W3 in Figure 9a).

In general, contact melting occurs at boundaries oriented at a high angle to the shortening direction. Although the mechanism of dissolution is not precisely known, the orientation of the contact melting boundaries suggests that higher normal stress on these boundaries are related directly (through elastic strain energy) or indirectly (through plastic strain energy) to contact melting.

Sliding on Crystal Boundaries

Sliding on the boundaries between crystals is active, regardless of the strain rate. Grain-boundary migration and contact melting have been observed as accommodation processes during sliding in slow strain-rate experiments. For example, grain-boundary sliding occurs along the grain boundary between the white phase crystals W1 and W2 between the stages Figure 9a. Sliding on the grain boundary is possible since the local space problem is solved by contact melting of W1 at the B1-W1 boundary. Grain-boundary migration also assists sliding (Figure 9a). The original sliding boundary (between W1 and W2) changes its orientation after grain-boundary migration, and further sliding becomes possible on the new grain boundary of a new orientation. Contact-melting-accommodated-sliding and grain-boundary-migration-assisted sliding allow large strains in the solid framework without internal deformation of the crystals.

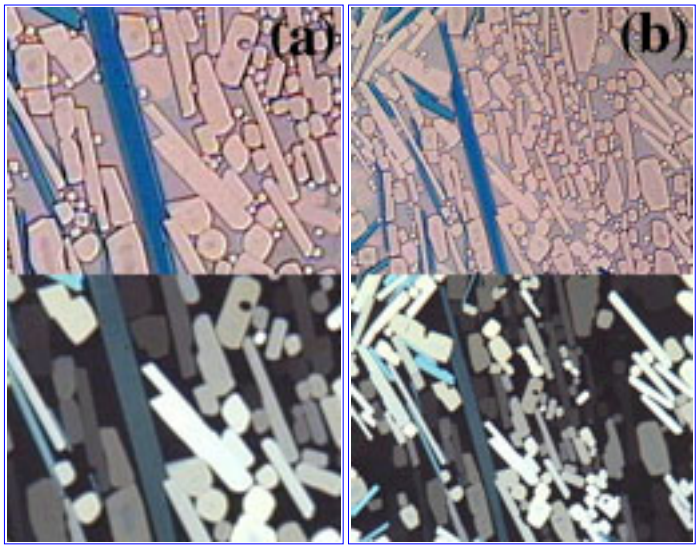

Figure 9. (a) Contact melting/redeposition during slow strain-rate experiment. W1,W2,W3: white phase crystals, B1: blue phase crystal. Elapsed time between the first and last frame= 100 minutes. Plane- and crossed-polarized light. Field width: 0.29 mm. (b) large-scale view of (a).

Filter Pressing

Two different types of filter pressing have been observed in our experiments; (1) filter

pressing which involves crystal plastic deformation with dynamic recrystallization (Figure 7), and (2) filter pressing which involves contact melting/redeposition and crystal-boundary sliding (Figure 8, 9b). When filter pressing occurs, a signature of the process is likely to be found in the spatial distribution of local chemical composition, since the melt, usually of different composition from the framework crystals, is removed during filter pressing. If filter pressing occurs during the early stage of crystallization, the formation of a nearly monominerallic rock or adcumulus is possible. If crystal plastic deformation and dynamic recrystallization are occurring during filter pressing, the resulting microstructures in the monominerallic part will be similar to the microstructures formed in solid-state deformation. Layers of igneous rocks which show strong evidence of crystal plastic deformation neighbored by less deformed or undeformed comagmatic igneous layers may indicate filter pressing at strain rates fast enough to operate deformation processes of crystal plasticity and dynamic recrystallization.

If cryptic processes such as contact melting and grain-boundary sliding are involved during filter pressing, the residual part will be undeformed-looking as shown in our experiments. Undeformed-looking adcumulus is commonly associated with large mafic intrusions and petrologists have been working on the problem of how the interstitial melt is removed from the adcumulus. Walker et al (1988) explain the formation of adcumulus with a zone refining model in which diffusion under a thermal gradient is involved. Since the liquid phase is removed by continuous reequilibration between interstitial melt and the main reservoir of magma by diffusion (Walker et al, 1988), the resulting crystal to crystal boundaries in the cumulate will be growth-impingement boundaries. However, when contact melting is involved during formation of adcumulus, the resulting crystal to crystal boundaries will be dissolution boundaries at which dissolution of one or two neighboring crystals occurred. Detailed petrographic work, including chemical imaging to see microstructures such as truncated zoning by grain or phase boundaries, may help to determine whether contact melting contributed to the formation of adcumulus.

Grain Flow

Grain flow or granular flow is a process similar to cataclastic flow in which most of strain is accommodated by sliding along boundaries and rotation of crystals. It is a term introduced by sedimentologists (Carter, 1975) for deformation of close-packed granular sediments with interstitial fluid, but it also seems to be appropriate for the present crystal/melt mixtures. Figure 10a shows accumulation of large shear strain (shearstrain>~5 between the first and last stage of Figure10a) of a solid framework by grain flow at a low melt fraction. Subparallel alignment of crystals to the flow plane (parallel to width of photomicrographs), resulting from rotation of crystals, is developed during deformation (near the last frame in Figure 10a). Significant localization of deformation is also observed to develop subparallel to the width of photomicrographs near the center of Figure 10a.

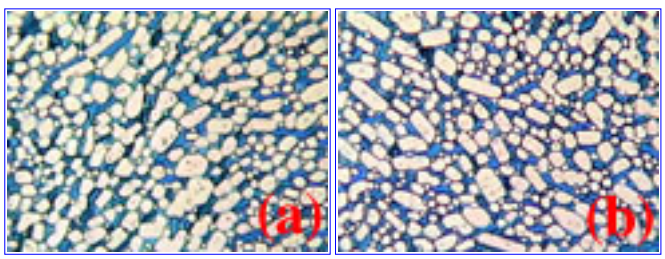

Figure 10. (a) Grain flow by sliding along crystal boundaries and rotation of crystals. Elapsed time between the first and last frame= 180 minutes. Plane-polarized light. Field width: 0.4

mm. (b) Development of a micro shear zone in the sample of low melt fraction. Elapsed time between the first and last frame= 180 minutes. Plane-polarized light. Field width: 0.4 mm.

When a solid framework is deforming by grain flow which involves grain-boundary sliding and rotation of crystals, a shape preferred orientation may develop by rigid body rotation of crystals and tiling effects (Tikoff & Teyssier, 1994). Preferred orientation of euhedral igneous minerals may be formed by rotation of crystals during grain flow even after formation of the solid framework, but since such shape preferred orientation is also possible by suspension flow or magmatic flow (Paterson et al, 1989), it is not always a reliable criterion for grain flow at low melt fraction. However, when all the phases present in a rock show shape preferred orientation instead of one phase, such shape preferred orientation can be more reliably interpreted as the result of grain flow at low melt fraction instead of suspension flow, since the melt fraction should be low to have multiple phases saturated in a normal magma system with a bulk composition close to the eutectic composition. However, this criterion should also be carefully applied, since there is a possibility that later crystallizing crystals can fill the interstitial spaces between the crystals with developed shape preferred orientation and may also show shape preferred orientation simply by mimicking the preexisting fabric.

Development of a Micro Shear Zone during Grain Flow

The term micro shear zone is used here for a zone with the width of one or two crystals where grain-boundary sliding is concentrated. An example from a sample of low melt fraction is shown in Figure 10b. It is noteworthy that such zones can develop without drawing melt into the zone. It is also remarkable that the micro shear zone (shaded region in Figure 10b) texturally closely resembles the surrounding regions. A cryptic kinematic domain of this kind would be difficult to recognize in rocks.

When a micro shear zone develops in a framework, recognition of such zones will be dependent on the nature of the zones. The resulting microstructure will be cryptic as observed from our experiments (Figure 10b), when a micro shear zone develops without change in the local melt fraction. However, when the melt fraction increases or decreases in a micro shear zone, melt drawn into the high strain zone or expelled from it will have a different chemistry compared to the whole rock, since the melt has a more evolved composition compared to the bulk composition of crystal-melt mixtures at the time of deformation. After crystallization, such melt zones during deformation will be the zones of slightly different mineral assemblages compared to the whole rock but in chemical equilibrium with the crystalline phases present in the neighboring region. Recognition of chemical equilibrium is important since a different mineral assemblage in such zones can also be formed by igneous veining or injection of a small dike.

Shearing during Heating

Melting experiments during deformation have been performed at melting rates slow enough relative to deformation rates to preserve a high proportion of the solid to solid contacts. Figure 11a is a time-lapse movie from a melting and deformation experiment. Melting of the blue phase crystals is most noticeable, but white and cube phase crystals are also melting. During melting, localized zone of deformation is developed near the area where large amount of melt is generated mostly by dissolution of the blue phase crystals. After complete melting of blue phase crystals, displacement impingement boundaries between white crystals form (the last frame of Figure 11a).

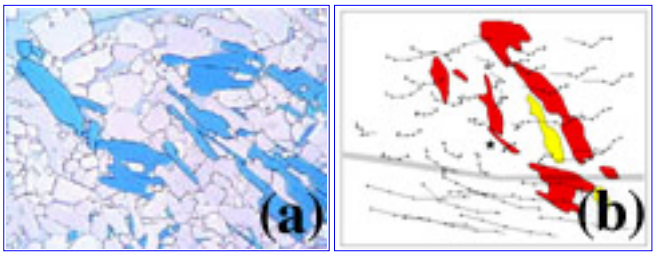

Figure 11. (a) Development of a high strain-rate zone during partial melting and sinistral shearing. Elapsed time between the first and last frame= 3 hours 49 minutes. Plane-polarized light. Field width: 0.4 mm. Thermal histories: 1st to 16th frame= 35 ºC, 37ºC, 38ºC, 39ºC, 40ºC, 41ºC, 42ºC, 43ºC, 44ºC, 45ºC, 46ºC, 47ºC, 48ºC, 49ºC, 50ºC, 51ºC. (b) Particle trajectories with superimposed blue phase crystal boundaries. Constructed from 11th to 16th frames, relative to the 11th frame. Squares represent the initial positions of material points. The red region represents the blue phase crystals at the initial stage for each particle trajectory. The yellow represents the blue phase crystals at the last stage for each displacement map.

The particle trajectories in Figure 11b are the trajectories constructed from the 11th to 16th frames after the 11th frame. The reference frame origin for the trajectory map is indicated by a star in Figure 11b, and horizontal edges of photomicrographs were used as one axis of an orthogonal reference frame. Above the subhorizontal high strain-rate zone that developed around the stage of the 6th frame in Figure 11a (also indicated as shaded region in Figure 11b), the direction of displacement vectors at the right and left edges on the map, points toward the origin, indicating some component of horizontal shortening. The shortening in the upper region is the result of blue phase crystal melting or the result of melt extraction and consequent displacement of white phase crystals. In the high strain-rate zone, an increase of the melt fraction is noticeable but no other textural feature distinguishes the zone from the more slowly straining material above it. Although it is not clear whether the extra melt in the zone is coming from the upper region or somewhere else, coincidence of the high melt fraction zone and the high strain-rate zone may suggest, firstly, development of the high strain-rate zone initiated by local melt fraction increase during melting, or secondly, melt drawn into the dilating high strain-rate zone as suggested by Hollister and Crawford (1986).

Previous Section Home Next Section

Discussion

The suggestions for interpretation of microstructures above were made based on observations in the analog experiments. Since the material property and conditions (e.g. strain rate and temperature) of the analog experimental system are very different from those of the natural geologic system, consideration of kinetic scaling (i.e. process rate scaling) as well as traditional mechanical scaling (e.g. length-, mass-, time- scaling) is necessary to confirm the suggested possibilities of microstructural evolution in natural systems. Microstructural similarity in different systems or conditions is achieved only when the history of relative rates among processes are identical (Park, 1994). Otherwise, the experiment is not properly scaled. Since the process rates at geological conditions are not known, it is impossible to know what the relative rates of processes should be in an analog system. For this reason, the significance of the experimental observations is not clear. Probably the best way of testing the possibilities suggested in this study is to study natural microstructures in detail. After detailed studies, the suggested possibilities can be accepted or rejected, depending on the presence or absence of suggested microstructures.

The processes observed in this system may or may not operate in natural magmatic system, depending on the process kinetics. If the rate of processes are slow even for geologic time (e.g. life span of a magma chamber), a reasonable conclusion is that processes with such a slow kinetics have no importance in changing the melt-grown igneous textures of rocks. But, how do we know whether the kinetics of processes are slow or fast in natural systems? The question can be answered by at least three different approaches. First, one can experimentally measure the process kinetics, using a real geological material. This will be possible only if a process is fast enough to occur on laboratory time scales (typically days to weeks). Second, one can test the possibility of a process by detailed petrographic studies. For example, a crystal which is made of one part which has grown from melt and another part which has grown by grain- or phase-boundary migration, may have slightly different chemical signature in these different parts which may be recognizable by detailed petrography with chemical imaging (e.g. Figure 5c). Finally, one can build a model (e.g. computer simulation) that links a process and the resulting textural change and check the time required for a process to change the texture. The possibility of a process can be accepted or rejected depending on the time required for textural change compared to times available for various processes in natural rock systems. Thus, the value of this type of experiments seems that the experiments can be sources of idea for setting up silicate experiments, petrographic works, and modelling.

Conclusions

From the analog experiments of textural development in igneous systems, the following possibilities are suggested for the evolution of textures in igneous rocks and interpretation of igneous textures.

(1) Segmentation of dendritic crystals may need to be considered as a new nucleation mechanism in some magmatic systems, especially the systems that experienced a rapid cooling. Segmented dendritic crystals may serve as growth centers around which the crystals grow, like conventional nuclei.

(2) Grain- or phase-boundary migration can change the geometry of boundaries such that older crystals appear younger. Caution must be exercised when inferring the order of crystallization after examining the geometry of crystal boundaries.

(3) Textural metamorphism in igneous rocks may start while the melt is present. This will make it difficult to interpret the textures in igneous rocks, and raises a question, "What is the proportion of primary melt-grown textures in igneous rocks?"

(4) During melt-present deformation of analog material, processes of crystal plastic deformation, dynamic recrystallization, contact melting/redeposition, and sliding along crystal boundaries, operate at the crystal scale, while deformation processes of filter pressing, grain flow, and localized deformation along micro shear zones, operate at the framework scale.

(5) When crystals deform by crystal plasticity during melt-present deformation, the resulting microstructural characteristics will be similar to those formed by solid-state crystal plastic deformation. If deformation ceased before complete crystallization, microstructures such as deformed crystals surrounded by undeformed minerals of igneous textures may be found.

(6) Where contact melting was a major deformation process, the resulting igneous rock may look optically strain-free. However, the presence of microstructural features such as preferred orientation of indented boundaries may indicate the deformation process of contact melting.

(7) Complete removal of melt by filter processing may be possible in igneous rocks by combined processes of crystal plastic deformation, contact melting, and crystal boundary sliding. Adcumulus may be formed by filter pressing in a crystallizing magma chamber where only one phase is saturated.

(8) Grain flow at a low melt fraction can form a preferred orientation of grain long axis. Thus, preferred orientation of igneous minerals may not always indicate high-melt fraction suspension type flow.

(9) When a solid framework deforms with localization along micro shear zones, recognition of the deformation process may be impossible. However, when such zones draw melt in or expel melt, it may be possible to recognize the localized deformation since these zones will have slightly different igneous mineral assemblages.

(10) It is observed from analog experiments that some deformation processes leave no signatures of deformation. Thus, estimation of deformation in igneous rocks, based on presence of crystal plastic deformation microstructures as in rocks deformed at solid state, may not be reliable.

ACKNOWLEDGMENTS

It has been my great pleasure to work and have numerous discussion sessions with Professor W.D. Means. I wish to thank my teacher for his support, encouragement and interest while this work was done at SUNY at Albany. I also wish to thank Mark Jessell, Paul Bons and Janos Urai for improving this manuscript and making this volume possible. This work was supported by NSF grants EAR-9017478, EAR-9204781 (equipment) & EAR-9404872 to W.D. Means.

Previous Section Home Next Section

References

Bosworth, W., 1981, Strain-induced preferential dissolution of halite, Tectonophysics, 78, pp. 509-525

Carter, R.M., 1975, A discussion and classification of subaqueous mass-transport with particular application to grain-flow, slurry flow, and fluxoturbidites. Earth Sci. Rev., 11, 145-177

Cashman, K.V. & Marsh, B.D., 1988, Crystal size distribution (CSD) in rocks and the kinetics and dynamics of crystallization. II. Makaopuhi lava lake, Contrib. Mineral. Petrol., 99, 292-305

Hollister, L.S. & Crawford, M.L., 1986, Melt-enhanced deformation: a major tectonic process, Geology, 14, pp. 558-561

Kahlweit, M., 1968, On the ageing of dendrites, Scripta. Metal., 2, 251-254

Kattamis, T.Z., Coughlin, J.C. & Flemings, M.C., 1967, Influence of coarsening on dendrite arm spacing of aluminum-copper alloys, Trans. Metal. Soc. AIME, 239, pp. 1604-1511

Lasaga, A.C., 1981, The atomistic basis of kinetics: defects in minerals, In: Kinetics of Geochemical Processes (eds. Lasaga, A.C. & Kirkpatrick, R.J.), Reviews in Mineralogy, volume 8, Mineralogical Society of America, pp. 261-320

Lofgren, G., 1980, Experimental studies on the dynamic crystallization of silicate melts, In: Physics of magmatic processes (ed. Hargraves, R.B.), Princeton, New Jersey, Princeton University Press, pp. 487-551

McBirney, A. R., 1993, Igneous petrology (2nd ed.). Jones and Bartlett Publishers, Inc., Boston, 508p.

Means, W.D. & Y. Park, 1994, New experimental approach to understanding igneous texture, Geology, 22, pp. 324-326

Park, Y., 1994, Microstructural evolution in crystal-melt systems, unpublished Ph.D. thesis, State Univ. of New York at Albany

Park, Y & Means, W.D., 1996, Direct observation of deformation processes in crystal mushes, J. Struct. Geol., 18, 847-858

Park, Y & Means, W.D., 1997, Crystal rotation and growth during grain flow in a deforming crystal mush, In: Evolution of Geologic Structures in Micro- to Macro-scales (ed. Sengupta, S.), Chapman & Hall, London, pp. 245-258

Paterson, S.R., Tobisch, O.T. & Vernon, R.H., 1991, Emplacement and deformation of granitoids during volcanic arc construction in the Foothills terrane, central Sierra Nevada, California, Tectonophysics, 191, pp. 89-110

Paterson, S.R., Vernon, R.H. & Tobisch, O.T., 1989, A review of criteria for the identification of magmatic and tectonic foliations in granitoids, J. Struct. Geol., 11, pp. 349-363

Ree, J.-H., 1991, High temperature deformation of octachlropropane: a microstructural study, unpublished Ph.D. thesis, State Univ. of New York at Albany

Robin, P.-Y.F., 1978, Pressure solution at grain-to-grain contacts, Geochim. Cosmochim. Acta, 42, pp. 1383-1389

Rostoker, W. & Dvorak, J.R., 1977, Interpretation of metallographic structures, New York, Academic Press, 250p.

Shannon, J.R., Walker, B.M., Carten, R.B. & Geraghty, E.P., 1982, Unidirectional solidification textures and their significance in determining relative ages of intrusions at the Henderson Mine, Colorado, Geology, 10, pp. 293-297

Shewmon, P.G., 1965, Metallurgical thermodynamics. In: Physical Metallurgy (ed. Cahn, R.W.), Amsterdam, North-Holland Publishing Company, 1100p.

Sprunt, E.S. & Nur, A., 1977, Experimental study of the effects of stress on solution rate, J. Geophys. Res., 82, pp. 3013-3022

Tegner, C., Wilson, J.L. & Brooks, C.K., 1993, Intraplutonic quench zones in the Kap Edvard Holm layered gabbro complex, East Greenland, J. Petrol., 34, 681-710

Tikoff, B. & Teyssier, C., 1994, Strain and fabric analyses based on porphyroblast interaction, J. Struct. Geol., 16, pp. 477-491

Urai, J.L., Means, W.D. & Lister, G.S., 1986, Dynamic recrytallization of minerals, In: Mineral and Rock Deformation: Laboratory Studies- The Paterson Volume (eds. Heard, H.C. & Hobbs, B.E.), Am. Geophys. Un. Geophys. Monogr., 36, 161-199

Walker, D., Jurewicz, S. & Watson, E.B., 1988, Adcumulus dunite growth in a laboratory thermal gradient, Contrib. Mineral. and Petrol., 99, pp. 306-319

Previous Section Home Next Section